https://doi.org/10.5194/cp-2021-185
Preprint. Discussion started: 5 January 2022

Climate of the Past Discussions

The use of paleoclimatic simulations to refine the environmental and chronological context of archaeological/paleontological sites.

Léa Terray[1], Masa Kageyama[2], Emmanuelle Stoetzel[3], Eslem Ben Arous[3,4,5], Raphaël Cornette[1] and Pascale Braconnot[2]

[1] Institut de Systématique, Evolution, Biodiversité (ISYEB) – UMR 7205, Muséum National d'Histoire Naturelle, CNRS, Sorbonne Université, EPHE, Université des Antilles, Paris, France.

[2] Laboratoire des Sciences du Climat et de l'Environnement (LSCE) – UMR 8212 / Institut Pierre Simon Laplace (IPSL) – UMR 8112, CEA/CNRS/UVSQ, Centre CEA-Saclay, Gif-sur-Yvette, France

[3] Histoire Naturelle de l'Homme Préhistorique (HNHP) – UMR 7194, CNRS, Muséum National d'Histoire Naturelle, Sorbonne Université, UPVD, Musée de l'Homme, Paris, France.

[4] Pan-African Evolution Research Group (Pan-Ev), Max Planck Institute for the Science of Human History, , Jena, Germany.

[5] Geochronology lab, Centro Nacional de Investigación sobre la Evolución Humana, Burgos, Spain

Correspondence to: Léa Terray (lea.terray@mnhn.fr)

https://doi.org/10.5194/cp-2021-185
Preprint. Discussion started: 5 January 2022

Climate of the Past Discussions

Abstract. To reconstruct the paleoenvironmental and chronological context of archaeological/paleontological sites is a key step to understand the evolutionary history of past organisms. Commonly used method to infer paleoenvironments rely on varied proxies such as faunal assemblages and isotopes. However, those proxies often show some inconsistencies. Regarding estimated ages of stratigraphic layers, they can vary depending on the dating method used. In this paper, we tested the potential of paleoclimate simulations to address this issue and contribute to the description of the environmental and chronological context of archaeological/paleontological sites. We produced a set of paleoclimate simulations corresponding to the stratigraphy of a Late-Pleistocene Holocene site, El Harhoura 2 (Morocco), and compared the climatic sequence described by these simulations to environmental inferences made from isotopes and faunal assemblages. Our results showed that in the studied site combined US-ESR ages were much more congruent with paleoenvironmental inferences than OSL ages. In addition, climatic variations were found to be more consistent with isotopic studies than faunal assemblages, allowing us to discuss unresolved discrepancies to date. This study illustrates the strong potential of our approach to refine the paleoenvironmental and chronological context of archaeological and paleontological sites.

https://doi.org/10.5194/cp-2021-185
Preprint. Discussion started: 5 January 2022


Climate of the Past Discussions

1 Introduction

Reconstruct paleoenvironments is a key step to understand the ecological context and evolutionary history of past organisms, and, hence, the link between their phenotype and the environment they lived in. Commonly used method to infer paleoenvironments rely on the organisms themselves, such as the qualitative presence/absence of species (e.g., Tchernov, 2002; Avery, 2007; Denys *et al.*, 2018), the association of certain taxa with their preferred modern habitat (e.g., Fernandez-Jalvo *et al.*, 1998; Stoetzel *et al.*, 2011), their relative abondances (e.g., Peters & Bork, 1999; Matthews, 2000; Belmaker & Hovers, 2011; Comay & Dayan, 2018) or variations in the amount of stable isotopes in organic tissues (Anderson and Arthur, 1983; Tieszen, 1991; Royer et al., 2013). Those approaches allow one to characterize the local environment in which organisms lived. However, drastic discrepancies can be observed between those proxies (e.g., Jeffrey, 2016; Davis & Pineda-Munoz, 2016). Relying on the chronological context can also help to understand global environmental conditions. However, depending on the dating method used, the age of the stratigraphic layers may vary and also lead to discrepancies in the chronoclimatic reconstructions (Ben Arous et al., 2020b).

Besides paleoenvironmental reconstructions, paleoclimate modeling is another field for which one of the objectives is to describe past environments. To do so, it simulates paleoclimates using physically based models that describe the dynamics and thermodynamics of the atmosphere, ocean, and continental and frozen surfaces coupled with water and carbon cycles. Those models efficiently describe the directions and large-scale patterns of past climate changes (Braconnot et al., 2012). They characterize past climates through quantified variables and have long been used to investigate past environmental changes (Kutzbach and Otto-Bliesner, 1982; Braconnot et al., 2012; Duplessy and Ramstein, 2013; Schmidt et al., 2014; Harrison et al., 2015). Conversely to paleoenvironment proxies, paleoclimate simulations are much influenced by large scale climate processes because they rely on the global dynamic of the Earth's climate system.

We propose to combine those two fields and to use climate simulations to discuss and refine the environmental and chronological context of El Harhoura 2 (EH2) cave, an archeological site located on the north-Atlantic coast of Morocco, whose microvertebrate assemblages have been extensively studied.

https://doi.org/10.5194/cp-2021-185
Preprint. Discussion started: 5 January 2022


Climate of the Past Discussions

What are the paleoclimate changes describe by climate simulations over the sequence at EH2? Are they consistent with paleoenvironmental inferences available in the literature made from faunal assemblages and isotopes? To answer these questions, we produced a set of climate simulations corresponding to EH2 stratigraphic layers. In order to discuss the chronological framework, we assessed the consistency between the climatic sequences describe by simulations according to the varied dating methods and paleoenvironmental proxies from previous studies, such as isotopes and faunal assemblages. We thus expected that the congruence between paleoclimate simulations and paleoenvironmental proxies will allow us to distinguish between those two dating hypotheses. We then discussed the previously raised discrepancies between the different paleoenvironmental proxies in the light of the results of climate simulations.

2 Material and methods

2.1 El Harhoura 2 cave

The archeological site EH2 is located on the Moroccan Atlantic coast in the Rabat-Témara region (33°57'08.9" N / 6°55'32.5" W). Dating, stratigraphic and paleoenvironmental information are summarized in **Fig1**. This site is dated from the Late Pleistocene to the mid-Holocene. Its stratigraphy is currently divided into 11 layers (each layer is abbreviated in "L" followed by the layer number), among which the first eight are well studied and considered in this paper. Those layers revealed an impressive taxonomic richness and delivered an important amount of large and small vertebrate remains (Michel et al., 2009; Stoetzel et al., 2011, 2012b). The site was used several time as a model to explore the relationship between the past diversity, the phenotype of organism and their environments (Stoetzel et al., 2010, 2011, 2012a, 2013, 2017; Campmas et al., 2015; Cornette et al., 2015; Terray et al., 2021).

At EH2, paleoenvironments have mainly been inferred based on two different kind of proxies: species presence and isotopes. Regarding species presence, environments were reconstructed using palaeoecological indices such as the Taxonomic habitat index (THI), which is a method based on the habitat preference of small vertebrates (Stoetzel, 2009; Stoetzel *et al.*, 2011, 2014). The presence and/or abundance of particular taxa can also be a strong indicator of certain types of environment, such as

https://doi.org/10.5194/cp-2021-185
Preprint. Discussion started: 5 January 2022


Climate of the Past Discussions

amphibians for humid context, or gerbils and gerboas for arid context. Isotope-based inferences were performed by Jeffrey (2016) on *Meriones* teeth from Layers 2 to 8 of EH2, providing varied indications about paleoenvironments such as aridity, relative humidity, seasonal variations and vegetal cover (Longinelli and Selmo, 2003; Navarro et al., 2004; Royer et al., 2013). Some inconsistencies were observed between species and isotopes based proxies on certain stratigraphic layers of the site (Jeffrey, 2016; Stoetzel *et al.*, 2019). On two layers (5 and 7), while THI indicates arid conditions, isotopes suggest a more humid and temperate climate. Given the mosaic-like landscape described at EH2 and the fact that the two methods do not record the same information (more global for faunal communities, at the scale of a limited number of individuals of a single species for isotopes), it is not surprising to meet some inconsistencies, but it makes it difficult to reliably infer the global environmental conditions of the site.

The current climatic context of EH2 is complex. Morocco, due to its geographical location, has a rich mosaic of climate types (Sobrino and Raissouni, 2000). In particular, the Rabat-Témara region where the cave is located is subject to climatic influences from the Atlantic Ocean in the west, the arid Sahara in the south and the Mediterranean region in the north. Its climate is marked by a strong annual and interannual irregularity with a hot and dry summer where precipitations are almost absent and evaporation is particularly high, and a soft and short winter with concentrated precipitations (Sobrino and Raissouni, 2000; Lionello et al., 2006). The site also suffered from important climatic fluctuations over time (e.g. Hooghiemstra *et al.*, 1992; deMenocal, 1995, 2004; Le Houérou, 1997; Carto *et al.*, 2009; Trauth, Larrasoaña, & Mudelsee, 2009; Drake *et al.*, 2011; Drake, Breeze, & Parker, 2013; Blome *et al.*, 2012; Kageyama *et al.*, 2013; Couvreur *et al.*, 2020). The Late Pleistocene - Holocene period (Marine Isotopic Stages (MIS) 5 to 1) is marked by significant global climate changes, which resulted in a succession of relatively humid/arid and open/closed environments at EH2 (Stoetzel, 2009; Stoetzel et al., 2011, 2012a, b). As a result, paleolandscapes of the Late Pleistocene are described as open steppe or savanna-like lands with patches of shrubs, woodlands and water bodies, the latter expanding during wet periods, especially during the mid-Holocene.

https://doi.org/10.5194/cp-2021-185
Preprint. Discussion started: 5 January 2022


Climate of the Past Discussions

All of the eight studied layers have been dated (Ben Arous et al., 2020b). Three different methods were used: OSL (Optical Stimulated Luminescence) (Jacobs and Roberts, 2012; Jacobs et al., 2012), combined US-ESR (combination of uranium series and electron spin resonance methods) (Janati-Idrissi et al., 2012; Ben Arous et al., 2020a) and AMS-^{14}C (radiocarbon dating) (Nespoulet and El Hajraoui, 2012; Marquer et al., *in press*). However, important discrepancies appear between methods when applied to a same layer, as for the L3 dated at approximately 40 ka using combined US-ESR and at 60 ka using OSL (**Fig1**). In addition, when two consecutive layers are dated with different methods, those dating can be inconsistent with the relative position of the layers as it is the case for the L6 dated at 108 ka using OSL and the L7 dated at 62 ka using combined US-ESR (**Fig1**).

Thus, two dating hypotheses emerge by combining dates consistent with the relative position of the layers. Those dating hypotheses are referred in this paper as DH1 and DH2 (DH for Dating Hypothesis) and are presented in **Fig1**.

https://doi.org/10.5194/cp-2021-185
Preprint. Discussion started: 5 January 2022

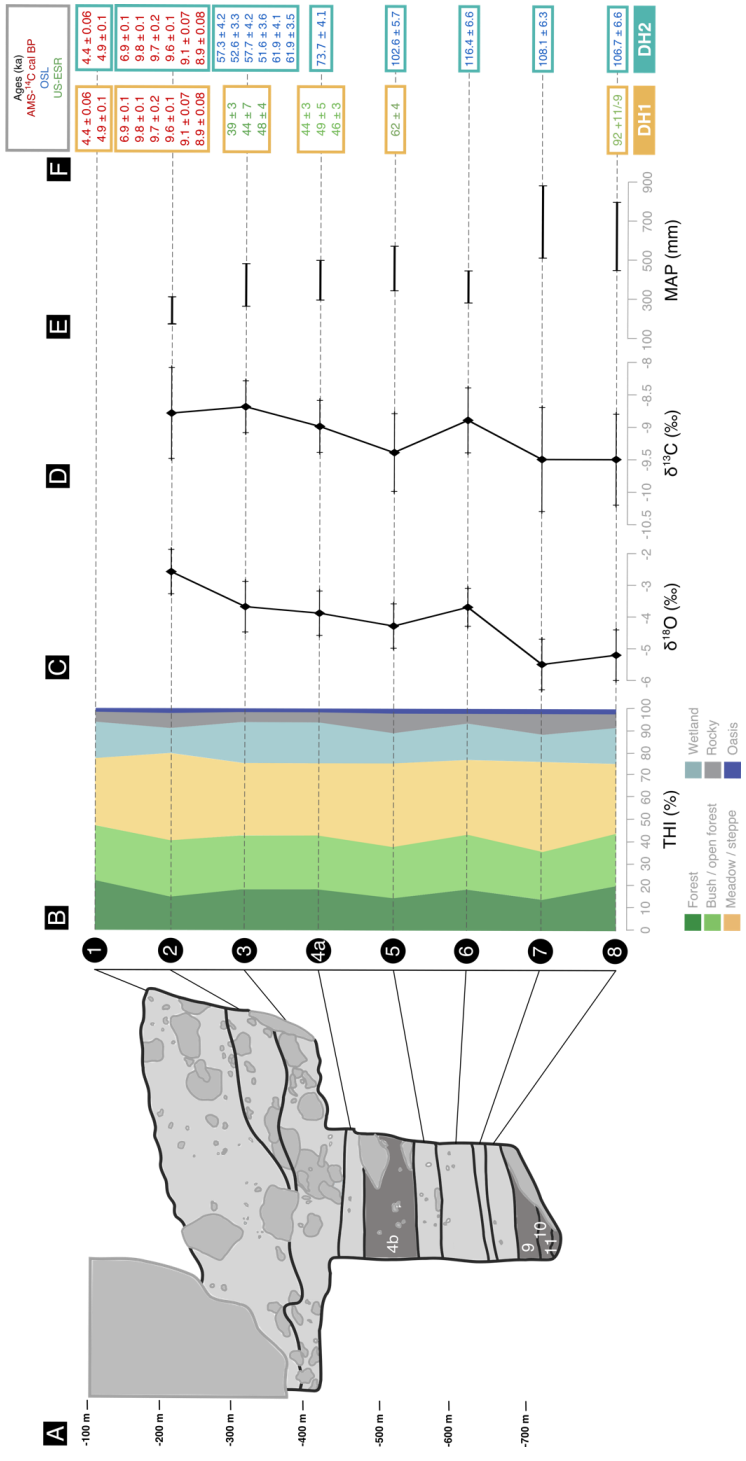

Fig. 1. Summary diagram displaying stratigraphy, paleoenvironmental proxies and the two dating hypotheses of El Harhoura 2 (EH2). A: stratigraphy of EH2, unused layers are in dark grey; B: relative % of THI values (adapted from Stoetzel *et al.* (2014) and Jeffrey (2016)); C: mean $\delta^{18}O$ values in *Meriones* teeth (from Jeffrey (2016)); D: mean $\delta^{13}C$ values in *Meriones* teeth (from Jeffrey (2016)); E: Mean Annual Precipitations (MAP; from Jeffrey (2016)); F: dating hypotheses DH1 and DH2 (Nespoulet and El Hajraoui, 2012; Jacobs et al., 2012; Janati-Idrissi et al., 2012; Ben Arous et al., 2020b, a; Marquer et al., *in press*).

https://doi.org/10.5194/cp-2021-185
Preprint. Discussion started: 5 January 2022


Climate of the Past Discussions

2.2 Paleoclimate simulations

2.2.1 Pre-existing ensemble of simulations

Climate simulations representative of key periods identified in EH2 layers were available to infer the climatic conditions at EH2. They have been run with different versions of the IPSL (IPSL for Institut Pierre-Simon Laplace) model (Marti et al., 2010; Dufresne et al., 2013; Boucher et al., 2020). All versions consider the full coupling between ocean, atmosphere, land-surface and sea-ice components, as well as an interactive carbon cycle. The exact complexity and resolution vary depending on model version. The different simulations also differ by Earth's orbit parameters, atmospheric trace gazes composition and ice sheet configurations in order to represent the climate conditions of the different periods (**Table1**). We used a total of six simulations:

- For the climate in L1 we used the reference midHolocene IPSL simulation (mean age estimated at ~6ka) run as part of the PMIP4-CMIP6 ensemble of simulations (Kageyama et al., 2017; Braconnot et al., 2021) .It is called *CM6mh* in the following and has been performed with IPSL-CM6A-LR (Boucher *et al.*, 2020). The atmosphere has a resolution of 144 points in longitude, 143 points in latitude and 79 vertical levels (144x143xL79). The ocean has a nominal 1°resolution with refined grid in the equatorial region and 75 vertical levels.
- For the climate in L2, L3 (DH1, DH2), L4a (DH1, DH2) and L5 (DH1) we used the *CM5AEH01* (early Holocene, mean age estimated at ~9ka), *MIS3mBB6* (mid-MIS3, mean age estimated at ~40ka), *MIS4dB6* (late MIS4, mean age estimated at ~60ka) and *MIS4mB6* (mid-MIS4, mean age estimated at ~66ka) simulations (Le Mézo et al., 2017) performed with IPSL-CM5A-LR (Dufresne et al., 2013). The model has a lower resolution that IPSL-CM6A-LR with 96 points in longitude, 96 points in latitude and 39 vertical levels (96x96xL39 in the following). The ocean grid is the orca 2 grid with 31 vertical levels.
- For the climate in L5 (DH2), L6 (DH2), L7 (DH2) and L8 (DH1, DH2) we used the *lig115k* simulation (MIS5d, mean age estimated at ~115ka) (Sicard personal communication) performed with IPSL-CM5A2-LR 96x96xL39 (Sepulchre et al., 2020). This model version is close to IPSL-CM5A-LR version and benefits from a retuning of the model to correct a model cold bias.

https://doi.org/10.5194/cp-2021-185
Preprint. Discussion started: 5 January 2022


Climate of the Past Discussions

Unfortunately, these simulations are not directly comparable because they were performed using different versions of the global coupled climate model. Indeed, those different versions, when used to simulate current climate, showed slightly different biases when compared to observations. This is due to the fact that the various versions of the model are characterized by different physical representations, resolutions and tuning. The differences between the collected simulations could then result from the difference in bias between the various versions of the model instead of representing climate differences between periods.

In order to make reliable comparisons between periods, we ran an entirely new set of simulations for the key periods of EH2: *midH* (for the mid-Holocene period), *earlyH* (for the early Holocene period), *midMIS3* (for the mid MIS3 period), *lateMIS4* (for the late MIS4 period), *midMIS4* (for the mid MIS4 period) and *MIS5d* (for the MIS5d period). Configurations information are summarized in **Table1**.

2.2.2 Model

We ran those new simulations using a unique model: LMDZOR6A. This model is a sub-configuration of the coupled model IPSL-CM6v1.11-LR, it considers the atmosphere-land surface component of the IPSL-CM6A-LR coupled model. It was chosen because it best simulates the climate on our area of interest (**SM Fig 1** and **2**). It also has the finest grid and improved representation of the atmospheric and land surface processes.

First, we produced a control simulation *Ctrl* on current days using the *clim_pdControl* experiment. This simulation is considered as the reference for the actual climate in our ensemble of simulations. Then, to produce other simulations, the same experimental set up as *Ctrl* was used. Orbital parameters, gaz concentrations, ice-sheet and other land-surface conditions were prescribes as in the corresponding coupled simulations. Boundary conditions files of pre-existing simulations were interpolated on the 143x144xL79 grid to be compatible with the grid of LMDZOR6A.

2.2.3 Sea-surface boundary conditions

https://doi.org/10.5194/cp-2021-185
Preprint. Discussion started: 5 January 2022


Climate of the Past Discussions

When using the atmospheric component alone the Sea Surface Temperature (SST) have to be forced. However, no SST reconstructions are available for the desired periods. Consequently, we imposed the simulated SST from pre-existing coupled simulations. However, those SST are also subjected to biases due to different model versions and they must be corrected. First, we estimated the differences between the SST biases of the three model versions. To do that we compared the SST simulated per each coupled model on current days with the SST of *clim_pdControl*. Those SST are the ones used for AMIP simulations (Atmospheric Model Intercomparison Project), which are a mean annual cycle of SST from observations. Secondly, we explored the consequences of those biases on the simulated climatology. We ran three test simulations *StanCM5ASST*, *StanCM5A2SST* and *StanCM6ASST*. They are similar to *Ctrl* except that we replaced the default SST (the SST of AMIP simulations) with the SST simulated per each of the three coupled model versions.

Finally, we computed the anomaly of each model version, i.e. the difference between the simulated SST and the SST used for AMIP simulations (issued from observations). For each coupled simulation, we corrected the simulated SST by the anomaly corresponding to the model version used. Corrected SST were obtained according to the formula:

$$SSTcor = SSTamip + (SSTsim - SSTmod)$$

Where SSTamip are the SST used for AMIP simulations, SSTsim the SST from the coupled simulation, SSTmod the SST of the model version for current days and SSTcor the corrected SST.

In total, the simulations ran for 50 years. Three monitoring variables were used: bils (surface total heat flux), nettop (net dn radiative flux at top of the atmosphere) and mrso (total soil moisture). Bils and nettop allow to ensure that the energy balance of the system has reach equilibrium, and mrso allow to verify the stabilization of the hydrological reservoir. In global the model reach equilibrium after eight years of simulation and at local scale on EH2 after 17 years (**SM Fig 3**). Consequently, we worked the last 30 years of each simulation.

https://doi.org/10.5194/cp-2021-185
Preprint. Discussion started: 5 January 2022

Table. 1. Forcing and boundary conditions of the ten simulations produced in this study.

	Ctrl	*Ctrl_CM6ASST*	*Ctrl_CM5ASST*	*Ctrl_CM5A2SST*	*H6k*	*H9k*	*P40k*	*P60k*	*P66k*	*P115k*
Initial simulation										
Name	-	-	-	-	CM6mh	CM5AEH01	MIS3mB6	MIS4dB6	MIS4mB6	lig155k
Model	-	-	-	-	IPSL-CM6A-LR	IPSL-CM5A-LR	IPSL-CM5A-LR	IPSL-CM5A-LR	IPSL-CM5A-LR	IPSL-CM5A2-LR
Date	Actual	Actual	Actual	Actual	~ 6 kyr BP	~ 9 kyr BP	~ 40 kyr BP	~ 60 kyr BP	~ 66 kyr BP	~ 115 kyr BP
Orbital parameters*										
Eccentricity	Same as *clim_pdControl*	Same as *clim_pdControl*	Same as *clim_pdControl*	Same as *clim_pdControl*	0.018682	0.01935	0.016715	0.024345	0.021311	0.041421
Obliquity (degrees)	Same as *clim_pdControl*	Same as *clim_pdControl*	Same as *clim_pdControl*	Same as *clim_pdControl*	24.105	24.231	23.441	22.391	22.493	22.404
Perihelion – 180	Same as *clim_pdControl*	Same as *clim_pdControl*	Same as *clim_pdControl*	Same as *clim_pdControl*	0.87	303.03	102.7	80.09	174.82	110.88
Solar constant (W/m2)	Same as *clim_pdControl*	Same as *clim_pdControl*	Same as *clim_pdControl*	Same as *clim_pdControl*	Same as *clim_pdControl*	Same as *clim_pdControl*	1365.6537	1365.6537	1365.6537	1361.20
Gaz concentration										
Carbon dioxide (ppm)	Same as *clim_pdControl*	Same as *clim_pdControl*	Same as *clim_pdControl*	Same as *clim_pdControl*	264	287	205	230	195	274
Methane (ppb)	Same as *clim_pdControl*	Same as *clim_pdControl*	Same as *clim_pdControl*	Same as *clim_pdControl*	597	791	500	450	450	505
Nitrous oxide (ppb)	Same as *clim_pdControl*	Same as *clim_pdControl*	Same as *clim_pdControl*	Same as *clim_pdControl*	262	275	260	230	217	251
SST	Same as *clim_pdControl*	tsol_oce from *CMIP6-IPSLCM6A-LR*	tsol_oce from *CMIP5-IPSLCM5A-MR*	tsol_oce from *CMIP6-IPSLCM5A2-LR*	tsol_oce from *CM6mh* (corrected)	tsol_oce from *CM5AEH01* (corrected)	tsol_oce from *MIS3mB6* (corrected)	tsol_oce from *MIS4dB6* (corrected)	tsol_oce from *MIS4mB6* (corrected)	tsol_oce from *lig115k* (corrected)
Geography	Same as *clim_pdControl*	Same as *clim_pdControl*	Same as *clim_pdControl*	Same as *clim_pdControl*	Same as *CM6mh*	Same as *CM5AEH01*	Same as *MIS3mB6*	Same as *MIS4dB6*	Same as *MIS4mB6*	Same as *lig115k*
Vegetation	Same as *clim_pdControl*	Same as *clim_pdControl*	Same as *clim_pdControl*	Same as *clim_pdControl*	Same as *CM6mh*	Same as *CM5AEH01*	Same as *MIS3mB6*	Same as *MIS4dB6*	Same as *MIS4mB6*	Same as *lig115k*

* The term "orbital parameters" refers to variations in the eccentricity of the Earth and longitude of perihelion as well as changes in its axial inclination (obliquity).

Climate of the Past Discussions
Open Access
EGU

https://doi.org/10.5194/cp-2021-185
Preprint. Discussion started: 5 January 2022


Climate of the Past Discussions

2.3 Climate variations through EH2 sequence

We then focused on describing the climate at EH2 cave and its variations over time according to the two dating hypotheses DH1 and DH2. To characterize the large scale climate over the area, we worked on the mean annual cycle of the four grid cells containing EH2. From simulations *Ctrl*, *midH*, *earlyH*, *midMIS3*, *lateMIS4*, *midMIS4* and *MIS5d* we extracted ten outputs variables that are likely to directly or indirectly (through available resources) influence organism's morphology. We selected: *tsol* (temperature at surface) (Gillooly et al., 2001; Yom-Tov and Geffen, 2006; Ebrahimi-Khusfi et al., 2020), *precip* (precipitations) (Yom-Tov and Geffen, 2006; Alhajeri and Steppan, 2016; Ebrahimi-Khusfi et al., 2020), *qsurf* (specific humidity) (Hovenden et al., 2012; Alhajeri and Steppan, 2016), *w10m* (wind at 10 meters) (Pellegrino et al., 2013; Chapman et al., 2011; Tanner et al., 1991; McNeil, 1991), *sols* (solar radiation at surface) (Monteith, 1972; Fyllas et al., 2017), *drysoil_frac* (fraction of visibly dry soil) (Paz et al., 2015) and *humtot* (total soil moisture) (Paz et al., 2015). Two additional variables were computed. The daily temperature amplitude *tsol_ampl_day* (Alhajeri and Steppan, 2016) computed from *tsol_max* (day maximum temperature) and *tsol_min* (day minimum temperature) as: *tsol_max – tsol_min*; and the hydric stress *hyd_stress* (Martínez-Blancas and Martorell, 2020) computed from *evapot* (potential evaporation) and *evap* (evaporation) as: *evapot – evap*. List of abbreviations and units is provided in **Table 2**. For each variable, we worked on a seasonal cycle averaged on the last 30 years of simulation. We explored variations in monthly means (mean value of the variable) and monthly standard deviations (amplitude of seasonal variation).

Table. 2. List of the climate variables used in this study, with their abbreviation and unit.

Short variable name	Complete variable name	Unit
tsol	temperature at surface	C°
tsol_ampl_day	daily temperature amplitude	C°
precip	precipitations	$mm.month^{-1}$

https://doi.org/10.5194/cp-2021-185
Preprint. Discussion started: 5 January 2022

qsurf	specific humidity	$kg.kg^{-1}$
w10m	wind at 10 meters	$m.s^{-1}$
sols	solar radiation at surface	$W.m^{-2}$
drysoil_frac	fraction of visibly dry soil	%
humtot	total soil moisture	$kg.m^{-2}$
hyd_stress	hydric stress	$mm.day^{-1}$

Climate variations over the EH2 sequence are presented on a common scale to ease the reading and better visualize covariation between climate variables (all variables were centered and reduced). In additions, to visualize climate proximity/differences between EH2 layers we performed principal component analyses (Jolliffe and Cadima, 2016). It allowed us to visualize EH2 layers into a climate-space by presenting the data along the principal components. These are new uncorrelated variables that successively maximize variance. They are computed from the eigenvectors and eigenvalues of the covariance/correlation matrix. The proximity of layers in the climate-space represents the similarity between the climate of the layers.

We tested the congruence between paleoenvironmental information available in the literature and our results from climatic simulations. As climate variables we used the principal components obtained before, and as paleoenvironmental proxies we used isotopes ($\delta^{18}O$ and $\delta^{13}C$) means (Jeffrey, 2016), reconstructed mean annual precipitations (Jeffrey, 2016) and percentages of represented habitats indicated by the THI (Stoetzel *et al.*, 2014) presented in **Fig1**. First, to test the global covariance between climate simulations and paleoenvironmental proxies we carried out two-block partial least squares (two-block PLS), a method for exploring the patterns of covariation between two sets of variables (Sampson et al., 1989; Streissguth et al., 1993). Then, to refine our results, we performed pairwise correlation tests. Regarding the THI, the oasis habitat was not tested because its percentage of presence does not vary over the EH2 sequence.

https://doi.org/10.5194/cp-2021-185
Preprint. Discussion started: 5 January 2022

All operations on netcdf files were performed using CDO (Climate Data Operators) (Schulzweida, 2019). Maps, plots and analyses were produced using the R free software (R Core Team, 2018) and the libraries *ncdf4* (http://dwpierce.com/software), *raster* (Hijmans and van Etten, 2012), *FactoMineR* (Lê et al., 2008), *corrplot* (Wei and Simko, 2021) and *ggplot2* (Wickham, 2015).

3 Results

3.1 Paleoclimate simulations

In **Fig2** we present the differences in SST biases between the three model versions. Regarding CM6A, there is a global cold bias up to 4°C and a hot bias in summer on the Mediterranean Sea compared to AMIP's SST. CM5A shows a rather homogeneous cold bias up to 6°C. As for CM5A2, the bias is more dependent of seasonality with a cold bias up to 5°C in winter and spring and a hot bias over Europe during summer and autumn.

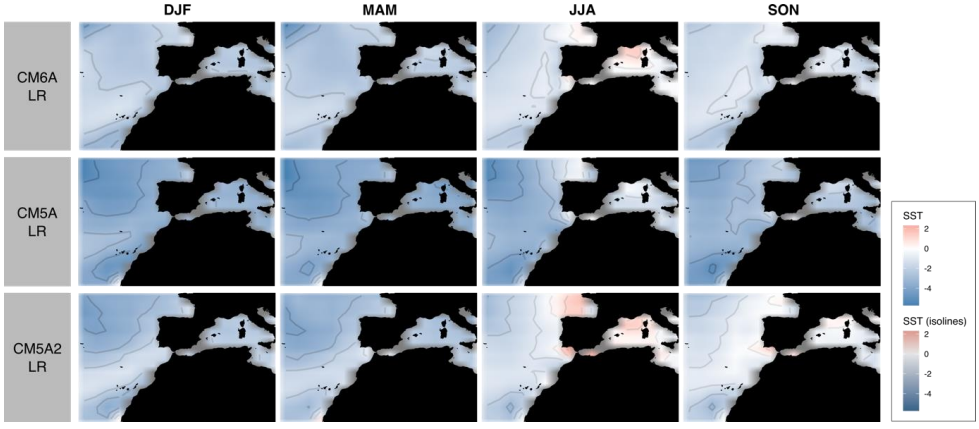

Fig. 2. Differences of sea surface temperature (SST) biases between IPSL-CM5A-LR, IPSL-CM5A2-LR and IPSL-CM6A-LR. SST of each model is presented in contrast with AMIP's SST (issued from observations). DJF: December, January, February (winter); MAM: March, April, May (spring); JJA: June, July, August (summer); SON: September, October, November (autumn).

https://doi.org/10.5194/cp-2021-185
Preprint. Discussion started: 5 January 2022

To assess in which extent differences in SST biases impact the simulated climate, maps and curves comparing outputs of *Ctrl* with outputs of *StanCM5ASST*, *StanCM5A2SST* and *StanCM6ASST* are presented in **Fig3** and **4**. We choose two metrics that are generally used to describe climatology: temperature (ts) and precipitations (pr) (Boucher et al., 2020). In each case a cold bias of ~5°C is observed over our area of interest. Some dry bias in precipitations are also noticed in winter. CM5 presents the strongest cold bias, up to 6 °C. CM5A2 display highly variable seasonal biases, with a cold one that reaches 6°C in winter and a hot one that reaches 2°C in summer. The climate simulated with the SST from CM6 is the closest to the climate simulated with the SST of AMIP.

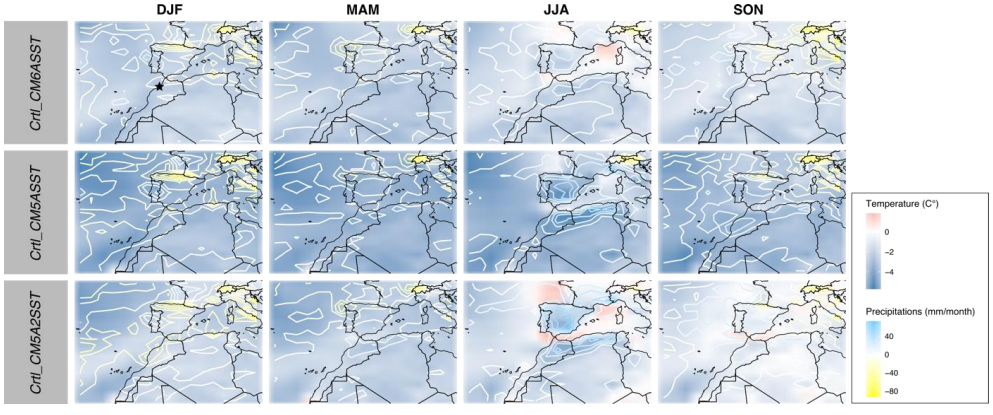

Fig. 3. Maps of EH2 region showing the impact of SST biases on the simulated climate. Temperature and precipitations simulated with *StanCM5ASST*, *StanCM5A2SST* and *StanCM6ASST* are presented in contrast with those of *Ctrl*. EH2 cave location is represented by the star. DJF: December, January, February (winter); MAM: March, April, May (spring); JJA: June, July, August (summer); SON: September, October, November (autumn).

https://doi.org/10.5194/cp-2021-185
Preprint. Discussion started: 5 January 2022

Climate of the Past Discussions
Open Access
EGU

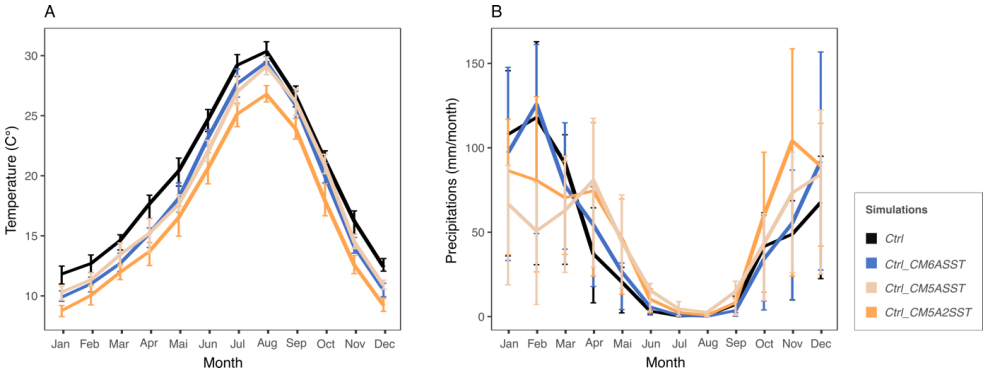

Fig. 4. Graph of seasonal variations in temperature and precipitations of *StanCM6ASST*, *StanCM5ASST*, *StanCM5A2SST* and *Ctrl* on the four grid cells containing EH2 cave. Interannual variation over the averaged 30 years is showed by quartiles.

Outputs of *midH*, *earlyH*, *midMIS3*, *lateMIS4*, *midMIS4* and *MIS5d* on the region of EH2 are presented in **Fig5**. Plots of monthly precipitations and temperatures are available in **Fig6**. From ~115ka until ~40ka, the climate was colder than currently with less and less seasonal variation. ~66ka and ~40ka are also marked by more important precipitations, especially in winter. Starting from ~9ka the seasonal temperature variation is more important. Conditions in winter and spring are similar to current climate, but a hotter autumn and a much warmer summer. At ~6ka, climate conditions are close from today, but with a slightly more important seasonal temperature variation. A one-month shift is observed in the annual maximum temperature between *Ctrl*, *midH*, *earlyH*, *lateMIS4*, *MIS5d* (maximum temperature reached in August) and *midMIS3*, *midMIS4* (maximum temperature reached in July). There are also important changes in the magnitude of the seasonal temperature variation from June to October and of the seasonal precipitation variation from October to May. Those tendencies are induced by differences in the obliquity of Earth's orbit and clearly separates interglacial climate (*Ctrl*, *midH*, *earlyH*) from glacial climate (*midMIS3*, *lateMIS4*, *midMIS4*, *MIS5d*).

https://doi.org/10.5194/cp-2021-185
Preprint. Discussion started: 5 January 2022

Climate of the Past Discussions
Open Access
EGU

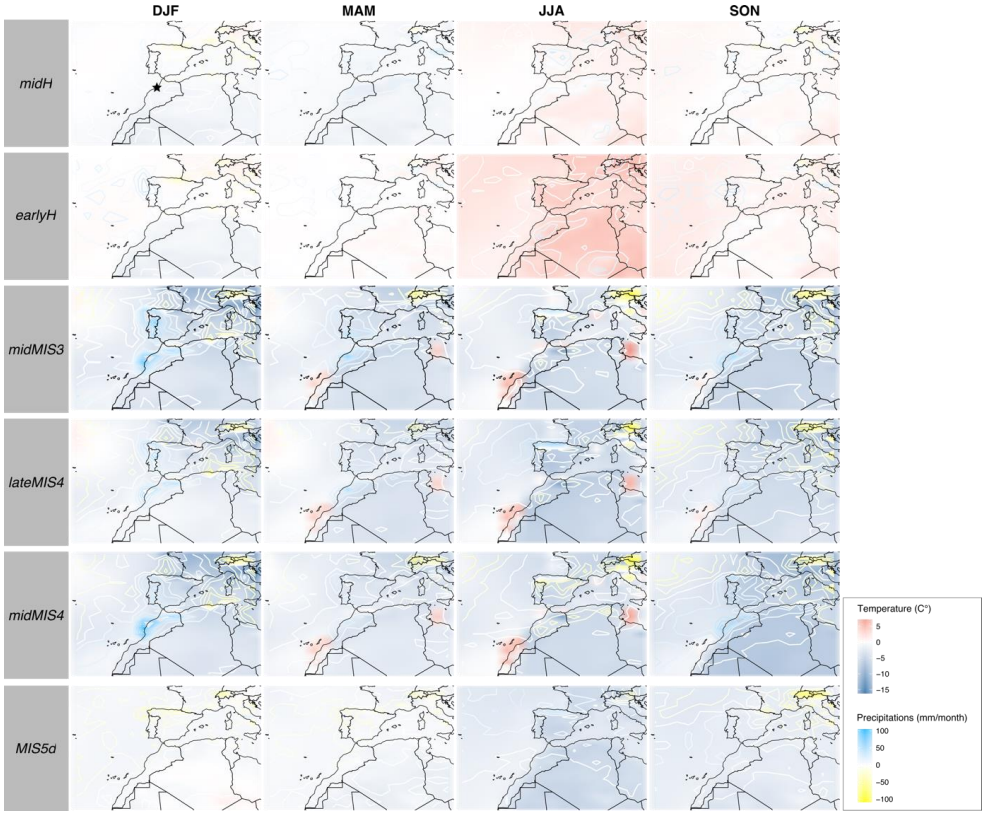

Fig. 5. Paleoclimatic reconstruction on EH2. Maps of temperature and precipitations simulated with *midH*, *earlyH*, *midMIS3*, *lateMIS4*, *midMIS4* and *MIS5d* are presented in contrast to *Ctrl* (the reference for actual climate in our dataset). EH2 cave location is represented by the star. DJF: December, January, February (winter); MAM: March, April, May (spring); JJA: June, July, August (summer); SON: September, October, November (autumn).

https://doi.org/10.5194/cp-2021-185
Preprint. Discussion started: 5 January 2022

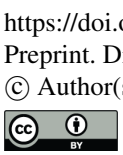

Climate of the Past Discussions
Open Access
EGU

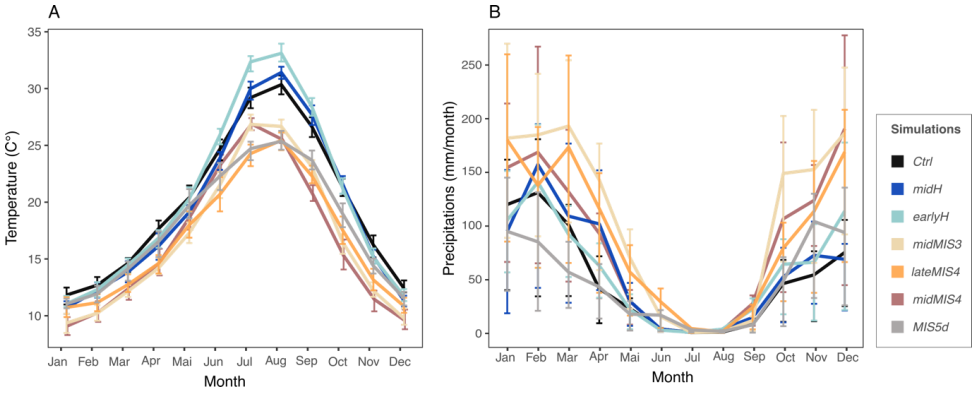

Fig. 6. Graph of monthly variations in temperature and precipitations on the four grid cells containing EH2 cave. Interannual variation over the averaged 30 years is visualized by quartiles.

3.2 Climate variations through EH2 sequence

Interpreting the results of paleoclimate simulations through the two dating hypotheses DH1 and DH2 allows us to describe hypothetic climatic changes over EH2 layers. Those two hypothetic climate sequences are presented in **Fig7**, the principal components analyses are showed in **Fig8**. To visualize how climate variables structure the climate-space of principal component analyses, biplots are available in **SM Fig 4.**

Based on DH1, our results indicate four major climate transitions (**Fig7**). The first occurs between L8 and L7. In L7 the climate is wetter and colder with more precipitations, soil humidity and wind, and less hydric stress and portions of dry soil. Humidity, precipitations and wind also show an important seasonal variability. The second transition, less marked, is between L6 and L4a. Climate in L4a is rather similar to climate in L6, but precipitations and humidity are increased. Seasonal variations are globally more pronounced. The third transition is between L3 and L2. The climate changes drastically, with more hot and drier conditions in L2. Temperature, solar radiations, water stress and soil dryness increase importantly, coupled with a decrease in the precipitations, soil moisture and wind. Specific humidity also increases strongly, which is consistent with the rise in temperature (the warmer the air is, the more water vaport it can contain, and thus the drier the soil).

https://doi.org/10.5194/cp-2021-185
Preprint. Discussion started: 5 January 2022


Climate of the Past Discussions

The last climatic transition, subtler, is between L1 and Act. The environment in Act seems close to the one in L8 with more seasonal variability in temperature, solar radiations and water stress.

Overall, it seems there is an alternation of two main climate types. This partition is confirmed by the principal component analysis showed in **Fig8**. The first principal component explains 65.85% of the observed variance and split the layers of EH2 into two climate groups. The first regroups L3, L4a, L6 and L7 and is defined by humid and windy conditions with a high seasonal variability. The second includes Act, L1, L2 and L8 and is characterized by hot and dry conditions. The second axis, explaining 30.28% of the variability, divides the latter group into two subgroups: L1 and L2 with high seasonal variability, and Act and L8 with a lower seasonal variability.

Regarding DH2, we observe three important climatic transitions (**Fig7**). The first happened between L5 and L4a. In L4a, the climate is much windier and temperature are colder with a substantial increase of daily temperature variations. Precipitations and soil moisture increase importantly while hydric stress decreases. The climate also presents an overall higher seasonal variability. These tendencies are even more pronounced in L3. The second transition is between L3 and L2. The soil is drier and the hydric stress increases greatly as well as solar radiations and temperatures. Precipitations and soil moisture are less important. Conditions in L1 are close from those in L2, a bit colder with a relatively less important water stress. The last climate transition, slighter than the previous ones, occurs between L1 and Act and is mainly marked by a global decrease of seasonal variation.

Results associated to DH2 suggest that three types of climates succeeded one another at EH2. The first group is composed of L8, L7, L6 and L5, the second by L3 and L4a and the third by L2, L1 and Act. As for DH1, this partition is supported by the principal component presented in **Fig8**. The first principal component, which explains 52.10% of the observed variance, separates the group containing L8, L7, L6 and L5 with the one composed L3 and L4a. The second principal component, explaining 42.35% of the observed variance, separates the group of L2, L1 and Act from others. L8, L7, L6 and L5 are characterized by a hot and dry climate and a low seasonal variation. L3 and L4a are defined by a wet and windy climate, with important precipitations and high seasonal variability. Finally, L2, L1 and Act present a hot environment associated with an important water stress.

https://doi.org/10.5194/cp-2021-185
Preprint. Discussion started: 5 January 2022

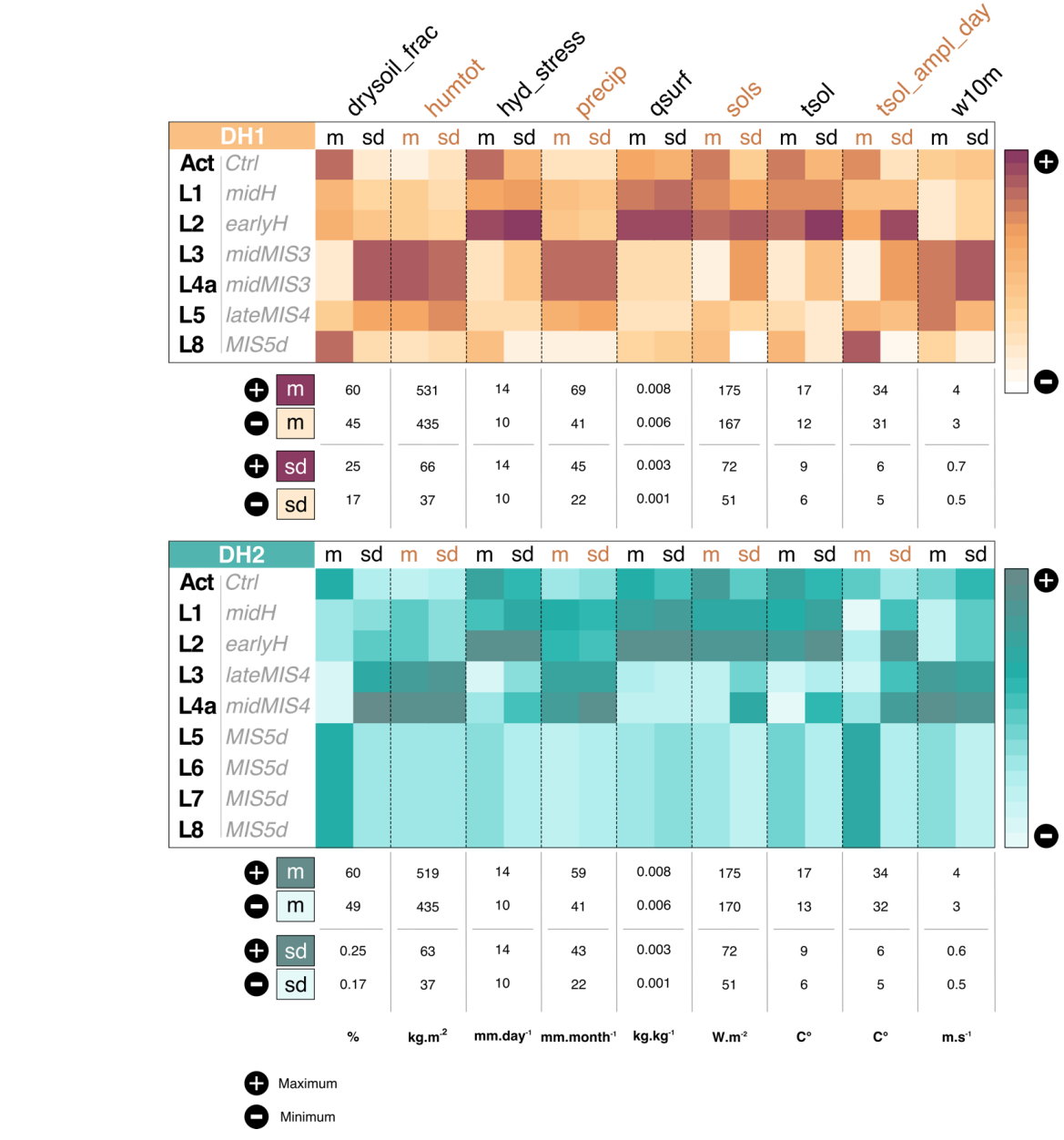

Fig. 7. Climatic variation over the EH2 sequence according to DH1 (Dating Hypothesis 1; upper), and DH2 (Dating Hypothesis 2; lower). Climate variables are centered and reduced and share a common scale. Maximum/minimum refers to the maximum/minimum value for all simulations. "L" is the abbreviation for Layer, "Act" for Actual, "m" for mean and "sd" for standard deviation.

https://doi.org/10.5194/cp-2021-185
Preprint. Discussion started: 5 January 2022

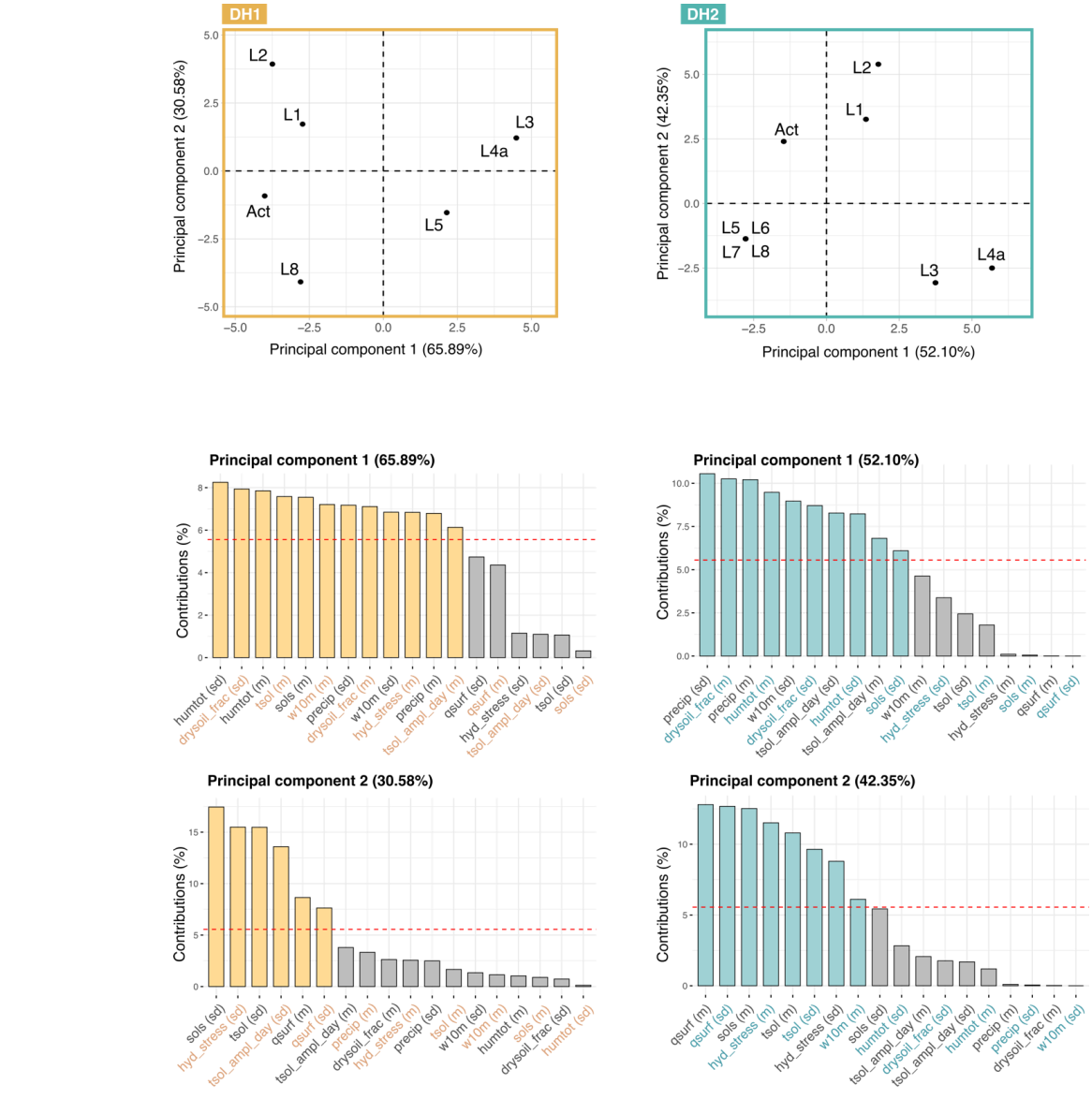

Fig. 8. Principal component analyses performed on climate variables according to DH1 (Dating Hypothesis 1; upper), and DH2 (Dating Hypothesis 2; lower). The contributions of climate variables to the two first principal components are presented (variables above the horizontal red line contribute significantly). "L" is the abbreviation for Layer and "Act" for Actual.

https://doi.org/10.5194/cp-2021-185
Preprint. Discussion started: 5 January 2022


Climate of the Past Discussions

Results of two-block PLS and correlations between climate variables and paleoenvironmental proxies are presented in **Fig9**. Regarding DH1, two-block PLS show that there is a statistically significant co-variation between THI values and all climate variables, and between isotope data and the principal component 2 (climate variables contributing to the principal component 2 are indicated in **Fig8**). Specifically, the principal component 2 is positively correlated with $\delta^{18}O$ mean, maximum and minimum values and $\delta^{13}C$ maximum values. Conversely, DH2 presents no statistically significant result for two-block PLS nor correlations.

https://doi.org/10.5194/cp-2021-185
Preprint. Discussion started: 5 January 2022

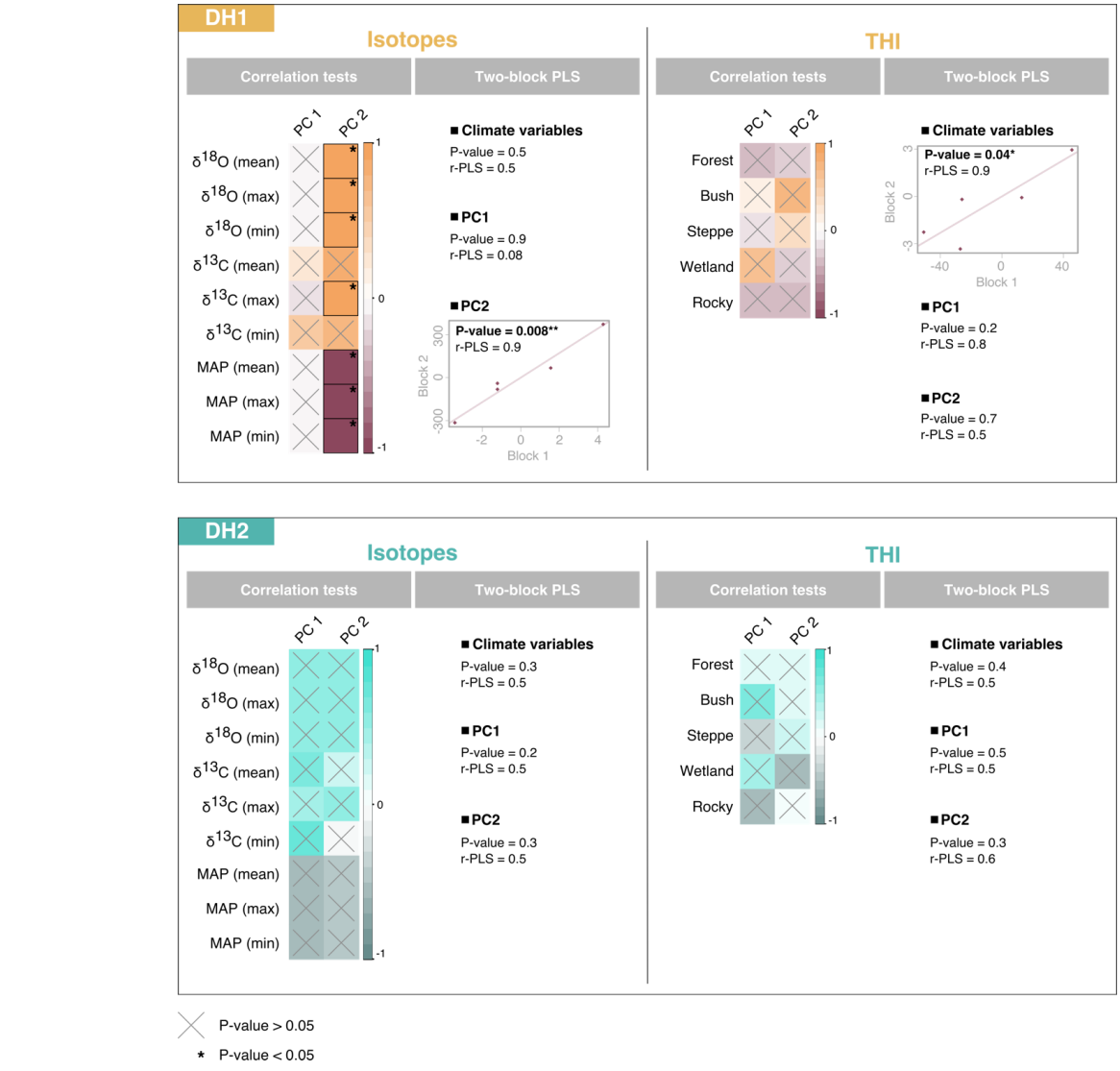

Fig. 9. Graphical representation of the two-block PLS and correlations between isotopes (Jeffrey, 2016) and THI values (Stoetzel et al., 2014) from the literature and climate variables according to DH1 (Dating Hypothesis 1; upper), and DH2 (Dating Hypothesis 2; lower). Crosses indicate cases where correlation is not significant (p-value > 0.05) and colors represent the strength of the correlations. "L" is the abbreviation for Layer, "m" for mean and "sd" for standard deviation. $\delta^{18}O$: mean $\delta^{18}O$ values in *Meriones* teeth (from Jeffrey (2016)); $\delta^{13}C$: mean $\delta^{13}C$ values in *Meriones* teeth (from Jeffrey (2016));

https://doi.org/10.5194/cp-2021-185
Preprint. Discussion started: 5 January 2022


Climate of the Past Discussions

MAP: Mean Annual Precipitations (from Jeffrey (2016)); Forest, Bush, Steppe, Wetland, Rocky: relative % of representation according to the THI (from Stoetzel *et al.* (2014) and Jeffrey (2016)).

4 Discussion

Paleoclimate simulations allow us to discuss several important climate changes at EH2 over the Late Pleistocene to mid-Holocene period. The described climate succession varies depending on the chronological framework. Regarding DH1, there is an alternation of two main climate types. The climate of L1, L2 and L8 is relatively similar to current climate, dry and hot with significant seasonal variation, defined as semi-arid. On the contrary, the climate of L3, L4a, L6 and L7, humid and colder with important and irregular precipitations, is more temperate. The succession revealed by DH2 is quite different, with the presence of three main climate types. The climate from L8 to L5 is dry, the climate of L3 and L4a is humid with important precipitations and the climate in L2, L1 and Act is semi-arid.

The climate sequences describe by DH1 and DH2 are not equally congruent with paleoenvironmental proxies from the literature. Indeed, several statistically significant correlations were found between the climate of DH1 and the paleoenvironmental proxies, while none were found for DH2. Then, our results suggest that, with respect to EH2, combined US-ESR dating may be more reliable than OSL dating. As this dating process rely on quartz grains and that their chronology and origin is difficult to establish in the context of karstic coastal caves (as discussed in Ben Arous *et al.*, 2020a), OSL ages might have been overestimated.

Isotopes are correlated to particular climate variables of DH1. Both $\delta^{18}O$ and $\delta^{13}C$ are mainly related to seasonal variation in temperature and water stress. It is known that a high amount of $\delta^{18}O$ is an indicator of aridity (Longinelli and Selmo, 2003; Levin et al., 2006). As the temperature increases, evaporation is more intense and because ^{16}O is a lighter isotope than ^{18}O, it will evaporate preferentially. Then the ratio between ^{16}O and ^{18}O changes, leading to an increase in the $\delta^{18}O$. It is then consistent to observe a $\delta^{18}O$ correlated with temperature and water stress. The $\delta^{13}C$ can reveal variations in the relative presence of C3, C4 and CAM plants (which refer to different metabolic carbon fixation pathway) because they have different signatures (O'Leary, 1988; Lin, 2013; Smiley et al., 2016). C3 plants are associated to

https://doi.org/10.5194/cp-2021-185
Preprint. Discussion started: 5 January 2022

375 temperate climate, C4 plants have an advantage in tropical environments (which is not the case here) and CAM are found in arid areas. Because CAM have greater $\delta^{13}C$ values than C3 plants, it is meaningful that higher $\delta^{13}C$ values are related to an increase in the seasonal variation of temperature and water stress. On the contrary to isotopes, related to particular climate variables, the THI is globally related to climate variations described by DH1. It is not surprising, as isotopes reveal fluctuations in particular 380 variables that are temperature and precipitations provided by a limited number of individuals of a single species, while THI is an estimate of the global type of the environment provided by the whole microvertebrate communities. Thus, they do not deliver information at the same resolution.

The large differences between the climate simulations and the fact that they provide a consistent view of the relationship between the different climatic variables allow us to discuss the inconsistencies 385 existing between paleoenvironmental proxies at EH2. The two major ones concern L5 and L7. In both cases, isotope surveys and mean annual precipitations reconstructions from Jeffrey (2016) indicate humid conditions with important precipitations. On the contrary, the THI as well as the presence of the steppic species *Jaculus* cf. *orientalis* (often used as an indicator of particularly arid conditions) and the scarcity of aquatic species support a dry climate (Stoetzel, 2009; Stoetzel et al., 2014). Large mammals 390 would also support this hypothesis, with an increase in the representation of gazelles and alcelaphines, and a decrease in the representation of bovines in both layers (Stoetzel et al., 2012a, 2014). Unfortunately, no combined US-ESR ages are available for L5 to date. Considering that climate conditions in L6 and L4a are humid with more important precipitations than currently, we could hypothesize a similar climate for L5. In that case, this would support isotope surveys. Nevertheless, we 395 cannot exclude that a microclimatic event could have induced particular climatic conditions on L5. Concerning L7, the climate describe by DH1 agrees with isotope surveys (Jeffrey, 2016). Those conclusions are supported by the increased abundance of *Crocidura russula*, a shrew species associated with Mediterranean climates (Cornette et al., 2015). In addition, *Jaculus* cf. *orientalis* can also be considered as an indicator of more continental conditions, such as the distance from the coastline, rather 400 than a marker of arid environments.

An important difference is noticed between the climate describe by DH1 and the THI. DH1 describes an arid climate on L1, in contradiction with the composition of small and large mammal communities

https://doi.org/10.5194/cp-2021-185
Preprint. Discussion started: 5 January 2022

that indicate a humid environment. This inconsistency could be explained by the location of EH2: the cave is subjected to a complex climatic influence, as described in section 2.1. Because global climate models describe general climate characteristics, in L1 the region could have been arid, but a local climate phenomenon could have generated a wet environment in the surroundings of EH2.

While our results seem conclusive, it is important to notice that our approach has some limitations. First, the climate model used has many forced parameters: sea ice temperature, aerosol concentration and vegetation are imposed to the model and not allowed to vary. Therefore, the vegetation feedback for example is not included in the model.

The second issue relates to the compatibility of the spatial and temporal resolution of a climate simulation and a stratigraphic layer of an archeological site. The spatial resolution of the atmospheric grid of the IPSL-CM6A-LR model is 157 km in average (Boucher et al., 2020). Consequently, the four cell grids used in this study cover a quite wide area. Conversely, EH2 represents a precise locality, and most species whose presence was recorded have a lifetime dispersal range largely inferior to 157km (e.g., the jird *Meriones shawii* has a home range estimated between 200-1000 m^2 (Ghawar et al., 2015)). Then, the climate described by simulations might be a bit too coarse to faithfully describe microclimate variations at EH2. This may induce a mismatch between climate variables and other paleoenvironmental proxies.

The difference in temporal resolution between a stratigraphic layer and a paleoclimate simulation raises even more concerns. The older the dated layer, the higher the dating uncertainty is. For EH2, this uncertainty goes until 11 ka on L8. If we compare the dates estimated by different methods, the difference is much more significant. For example, it is the case for L3 dated at ~40 ka by combined US-ESR and at ~60 by OSL (i.e. a difference of 20 ka). Radical climate changes can occur in 20 ka: ~60 ka places L3 in the last ice age while ~40 ka places it in the interglacial. As this paper demonstrates by comparing DH1 and DH2, those differences in estimated dates can result in completely different climate sequence. EH2 was an ideal case because a lot of studies focusing on the dating of its stratigraphic layers are found in the literature (e.g., Jacobs *et al.*, 2012; Janati-Idrissi *et al.*, 2012; Ben Arous *et al.*, 2020a,b). However, for archeological and paleontological sites, whose chronological framework is less referenced, it can lead to a completely wrong climate description. Furthermore, layers are not necessarily

https://doi.org/10.5194/cp-2021-185
Preprint. Discussion started: 5 January 2022

snapshots representing the faunal assemblages, cultural presence, etc. of specific moments in the past. A layer is a stratigraphic/sedimentary unit that can cover more or less long periods and undergo microclimatic variations that cannot be disentangled.

5 Conclusion

The use of climate simulations allowed us to provide a quantify description of the paleoclimate at El Harhoura 2. Our results enabled to discuss the varied dating methods used: in our case, the climate sequence corresponding to combined US-ESR ages was much more consistent with paleoenvironmental inferences than that corresponding to OSL ages. Regarding discrepancies between paleoenvironmental inferences based on faunal assemblages and isotopic studies, our results are more consistent with conclusions drawn from the latter. But more than that, they highlighted the difference in scale between the information provided by each of these indicators. This study demonstrates that the combination of different sources of environemental data and climate simulations has a great potential for refining paleoenvironmental and chronological context of archeological and paleontological sites.

Code and data availability

The code and data used in this article are available on reasonnable request to the corresponding author.

Author contribution

Conceptualization: Léa Terray, Pascale Braconnot, Raphaël Cornette, Emmanuelle Stoetzel.

Formal analyses: Léa Terray.

Methodology: Léa Terray, Pascale Braconnot, Masa Kageyama.

Funding acquisition: Léa Terray.

Writing – original draft preparation: Léa Terray.

Writing – review & editing: Pascale Braconnot, Emmanuelle Stoetzel, Eslem Ben Arous.

Competing interests

https://doi.org/10.5194/cp-2021-185
Preprint. Discussion started: 5 January 2022

The authors declare that they have no conflict of interest.

Acknowledgments

The microvertebrate remains from El Harhoura 2 cave were recovered and studied within the framework of the El Harhoura-Témara Archaeological Mission (dir. R. Nespoulet and M.A. El Hajraoui), under the administrative supervision of the *Institut National des Sciences de l'Archéologie et du Patrimoine* (Rabat, Morocco) and financial support from the *Ministère des Affaires Etrangères et du Développement International* (France) and the *Ministère de la Culture* (Maroc). The authors would like to thank Marie Sicard for sharing the *lig115* climate simulation, part of her PhD project. We also thank Amy Jeffrey, Julia Lee-Thorp and Nick Barton for allowing us to use the isotopic data from El Harhoura 2. Climate simulations were carried out on the Jean Zay supercomputer at IDRIS and the computing time was provided by the project nfl. This research was funded by the Université 463 Paris Descartes, the Ecole Doctorale FIRE – Programme Bettencourt.

https://doi.org/10.5194/cp-2021-185
Preprint. Discussion started: 5 January 2022

References

Adler, R., Sapiano, M., Huffman, G., Wang, J.-J., Gu, G., Bolvin, D., Chiu, L., Schneider, U., Becker, A., Nelkin, E., Xie, P., Ferraro, R., and Shin, D.-B.: The Global Precipitation Climatology Project (GPCP) Monthly Analysis (New Version 2.3) and a Review of 2017 Global Precipitation, Atmosphere, 9, 138, https://doi.org/10.3390/atmos9040138, 2018.

Alhajeri, B. H. and Steppan, S. J.: Association between climate and body size in rodents: A phylogenetic test of Bergmann's rule, Mamm. Biol., 81, 219–225, https://doi.org/10.1016/j.mambio.2015.12.001, 2016.

Anderson, T. F. and Arthur, M. A.: Stable isotopes of oxygen and carbon and their application to sedimentological and palaeoenvironmental problems., in: Stable Isotopes in Sedimentary Geochemistry: Society of Economic Palaeontologists and Mineralogists Short course, Vol. 10, edited by: Arthur, M. A., Anderson, T. F., Kaplan, I. R., Veizer, J., and Land, L. S., 1.1-1–151, 1983.

Avery, D. M.: Pleistocene micromammals from Wonderwerk Cave, South Africa: practical issues, J. Archaeol. Sci., 34, 613–625, https://doi.org/10.1016/j.jas.2006.07.001, 2007.

Belmaker, M. and Hovers, E.: Ecological change and the extinction of the Levantine Neanderthals: implications from a diachronic study of micromammals from Amud Cave, Israel, Quat. Sci. Rev., 30, 3196–3209, https://doi.org/10.1016/j.quascirev.2011.08.001, 2011.

Ben Arous, E., Falguères, C., Tombret, O., El Hajraoui, M. A., and Nespoulet, R.: Combined US-ESR dating of fossil teeth from El Harhoura 2 cave (Morocco): New data about the end of the MSA in Temara region, Quat. Int., 556, 88–95, https://doi.org/10.1016/j.quaint.2019.02.029, 2020a.

Ben Arous, E., Falguères, C., Nespoulet, R., and El Hajraoui, M. A.: Review of chronological data from the Rabat-Temara caves (Morocco): Implications for understanding human occupation in north-west Africa during the Late Pleistocene., in: Not just a corridor. Human occupation of the Nile Valley and neighbouring regions between 75,000 and 15,000 years ago, edited by: Leplongeon, A., Goder-Goldberger, M., and Pleurdeau, D., Paris, 177–201, 2020b.

Berrisford, P., Dee, D., Poli, P., Brugge, R., Fielding, M., Fuentes, M., Kållberg, P., Kobayashi, S., Uppala, S., and Simmons, A.: The ERA-Interim archive Version 2.0, ERA Report Series, 2011.

Blome, M. W., Cohen, A. S., Tryon, C. A., Brooks, A. S., and Russell, J.: The environmental context for the origins of modern human diversity: A synthesis of regional variability in African climate 150,000–30,000 years ago, J. Hum. Evol., 62, 563–592, https://doi.org/10.1016/j.jhevol.2012.01.011, 2012.

Boucher, O., Servonnat, J., Albright, A. L., Aumont, O., Balkanski, Y., Bastrikov, V., Bekki, S., Bonnet, R., Bony, S., Bopp, L., Braconnot, P., Brockmann, P., Cadule, P., Caubel, A., Cheruy, F., Codron, F., Cozic, A., Cugnet, D., D'Andrea, F., Davini, P., Lavergne, C., Denvil, S., Deshayes, J., Devilliers, M., Ducharne, A., Dufresne, J., Dupont, E., Éthé, C., Fairhead, L., Falletti, L., Flavoni, S., Foujols, M., Gardoll, S., Gastineau, G., Ghattas, J., Grandpeix, J., Guenet, B., Guez, L., E., Guilyardi, E., Guimberteau, M., Hauglustaine, D., Hourdin, F., Idelkadi, A., Joussaume, S., Kageyama, M., Khodri, M., Krinner, G., Lebas, N., Levavasseur, G., Lévy, C., Li, L., Lott, F., Lurton, T., Luyssaert, S., Madec, G., Madeleine, J., Maignan, F., Marchand, M., Marti, O., Mellul, L., Meurdesoif, Y., Mignot, J., Musat, I., Ottlé, C., Peylin, P., Planton, Y., Polcher, J., Rio, C., Rochetin, N., Rousset, C., Sepulchre, P., Sima, A., Swingedouw, D., Thiéblemont, R., Traore, A. K., Vancoppenolle, M., Vial, J., Vialard, J., Viovy, N., and Vuichard, N.: Presentation and Evaluation of the IPSL-CM6A-LR Climate Model, J. Adv. Model. Earth Syst., 12, https://doi.org/10.1029/2019MS002010, 2020.

Braconnot, P., Harrison, S. P., Kageyama, M., Bartlein, P. J., Masson-Delmotte, V., Abe-

https://doi.org/10.5194/cp-2021-185
Preprint. Discussion started: 5 January 2022

Ouchi, A., Otto-Bliesner, B., and Zhao, Y.: Evaluation of climate models using palaeoclimatic data, Nat. Clim. Change, 2, 417–424, https://doi.org/10.1038/nclimate1456, 2012.

Braconnot, P., Albani, S., Balkanski, Y., Cozic, A., Kageyama, M., Sima, A., Marti, O., and Peterschmitt, J.-Y.: Impact of dust in PMIP-CMIP6 mid-Holocene simulations with the IPSL model, Clim. Past, 17, 1091–1117, https://doi.org/10.5194/cp-17-1091-2021, 2021.

Campmas, E., Michel, P., Costamagno, S., Amani, F., Stoetzel, E., Nespoulet, R., and El Hajraoui, M. A.: Were Upper Pleistocene human/non-human predator occupations at the Témara caves (El Harhoura 2 and El Mnasra, Morocco) influenced by climate change?, J. Hum. Evol., 78, 122–143, https://doi.org/10.1016/j.jhevol.2014.08.008, 2015.

Carto, S. L., Weaver, A. J., Hetherington, R., Lam, Y., and Wiebe, E. C.: Out of Africa and into an ice age: on the role of global climate change in the late Pleistocene migration of early modern humans out of Africa, J. Hum. Evol., 56, 139–151, https://doi.org/10.1016/j.jhevol.2008.09.004, 2009.

Chapman, J. W., Klaassen, R. H. G., Drake, V. A., Fossette, S., Hays, G. C., Metcalfe, J. D., Reynolds, A. M., Reynolds, D. R., and Alerstam, T.: Animal Orientation Strategies for Movement in Flows, Curr. Biol., 21, R861–R870, https://doi.org/10.1016/j.cub.2011.08.014, 2011.

Comay, O. and Dayan, T.: From micromammals to paleoenvironments, Archaeol. Anthropol. Sci., 10, 2159–2171, https://doi.org/10.1007/s12520-018-0608-8, 2018.

Cornette, R., Stoetzel, E., Baylac, M., Moulin, S., Hutterer, R., Nespoulet, R., El Hajraoui, M. A., Denys, C., and Herrel, A.: Shrews of the genus Crocidura from El Harhoura 2 (Témara, Morocco): The contribution of broken specimens to the understanding of Late Pleistocene–Holocene palaeoenvironments in North Africa, Palaeogeogr. Palaeoclimatol. Palaeoecol., 436, 1–8, https://doi.org/10.1016/j.palaeo.2015.06.020, 2015.

Couvreur, T. L. P., Dauby, G., Blach-Overgaard, A., Deblauwe, V., Dessein, S., Droissart, V., Hardy, O. J., Harris, D. J., Janssens, S. B., Ley, A. C., Mackinder, B. A., Sonké, B., Sosef, M. S. M., Stévart, T., Svenning, J., Wieringa, J. J., Faye, A., Missoup, A. D., Tolley, K. A., Nicolas, V., Ntie, S., Fluteau, F., Robin, C., Guillocheau, F., Barboni, D., and Sepulchre, P.: Tectonics, climate and the diversification of the tropical African terrestrial flora and fauna, Biol. Rev., 96, 16–51, https://doi.org/10.1111/brv.12644, 2020.

Davis, M. and Pineda-Munoz, S.: The temporal scale of diet and dietary proxies, Ecol. Evol., 6, 1883–1897, https://doi.org/10.1002/ece3.2054, 2016.

deMenocal, P. B.: Plio-Pleistocene African Climate, Science, 270, 53–59, https://doi.org/10.1126/science.270.5233.53, 1995.

deMenocal, P. B.: African climate change and faunal evolution during the Pliocene–Pleistocene, Earth Planet. Sci. Lett., 220, 3–24, https://doi.org/10.1016/S0012-821X(04)00003-2, 2004.

Denys, C., Stoetzel, E., Andrews, P., Bailon, S., Rihane, A., Huchet, J. B., Fernandez-Jalvo, Y., and Laroulandie, V.: Taphonomy of Small Predators multi-taxa accumulations: palaeoecological implications, Hist. Biol., 30, 868–881, https://doi.org/10.1080/08912963.2017.1347647, 2018.

Drake, N. A., Blench, R. M., Armitage, S. J., Bristow, C. S., and White, K. H.: Ancient watercourses and biogeography of the Sahara explain the peopling of the desert, Proc. Natl. Acad. Sci., 108, 458–462, https://doi.org/10.1073/pnas.1012231108, 2011.

Drake, N. A., Breeze, P., and Parker, A.: Palaeoclimate in the Saharan and Arabian Deserts during the Middle Palaeolithic and the potential for hominin dispersals, Quat. Int., 300, 48–61, https://doi.org/10.1016/j.quaint.2012.12.018, 2013.

Dufresne, J.-L., Foujols, M.-A., Denvil, S., Caubel, A., Marti, O., Aumont, O., Balkanski, Y., Bekki, S., Bellenger, H., Benshila, R., Bony, S., Bopp, L., Braconnot, P., Brockmann, P.,

https://doi.org/10.5194/cp-2021-185
Preprint. Discussion started: 5 January 2022

Cadule, P., Cheruy, F., Codron, F., Cozic, A., Cugnet, D., de Noblet, N., Duvel, J.-P., Ethé, C., Fairhead, L., Fichefet, T., Flavoni, S., Friedlingstein, P., Grandpeix, J.-Y., Guez, L., Guilyardi, E., Hauglustaine, D., Hourdin, F., Idelkadi, A., Ghattas, J., Joussaume, S., Kageyama, M., Krinner, G., Labetoulle, S., Lahellec, A., Lefebvre, M.-P., Lefevre, F., Levy, C., Li, Z. X., Lloyd, J., Lott, F., Madec, G., Mancip, M., Marchand, M., Masson, S., Meurdesoif, Y., Mignot, J., Musat, I., Parouty, S., Polcher, J., Rio, C., Schulz, M., Swingedouw, D., Szopa, S., Talandier, C., Terray, P., Viovy, N., and Vuichard, N.: Climate change projections using the IPSL-CM5 Earth System Model: from CMIP3 to CMIP5, Clim. Dyn., 40, 2123–2165, https://doi.org/10.1007/s00382-012-1636-1, 2013.

Duplessy, J.-C. and Ramstein, G.: Paléonclimatologie, tome II : enquêter sur les climats anciens., CNRS Editions., 2013.

Ebrahimi-Khusfi, Z., Mirakbari, M., and Khosroshahi, M.: Vegetation response to changes in temperature, rainfall, and dust in arid environments, Environ. Monit. Assess., 192, 691, https://doi.org/10.1007/s10661-020-08644-0, 2020.

Fernandez-Jalvo, Y., Denys, C., Andrews, P., Williams, T., Dauphin, Y., and Humphrey, L.: Taphonomy and palaeoecology of Olduvai Bed-I (Pleistocene, Tanzania), J. Hum. Evol., 34, 137–172, 1998.

Fyllas, N. M., Bentley, L. P., Shenkin, A., Asner, G. P., Atkin, O. K., Díaz, S., Enquist, B. J., Farfan-Rios, W., Gloor, E., Guerrieri, R., Huasco, W. H., Ishida, Y., Martin, R. E., Meir, P., Phillips, O., Salinas, N., Silman, M., Weerasinghe, L. K., Zaragoza-Castells, J., and Malhi, Y.: Solar radiation and functional traits explain the decline of forest primary productivity along a tropical elevation gradient, Ecol. Lett., 20, 730–740, https://doi.org/10.1111/ele.12771, 2017.

Ghawar, W., Zaätour, W., Chlif, S., Bettaieb, J., Chelghaf, B., Snoussi, M.-A., and Salah, A. B.: Spatiotemporal dispersal of Meriones shawi estimated by radio-telemetry, Int. J. Multidiscip. Res. Dev., 2, 211–216, 2015.

Gillooly, J. F., Brown, J. H., West, G. B., Savage, V. M., and Charnov, E. L.: Effects of Size and Temperature on Metabolic Rate, Science, 293, 2248–2251, 2001.

Harrison, S. P., Bartlein, P. J., Izumi, K., Li, G., Annan, J., Hargreaves, J., Braconnot, P., and Kageyama, M.: Evaluation of CMIP5 palaeo-simulations to improve climate projections, Nat. Clim. Change, 5, 735–743, https://doi.org/10.1038/nclimate2649, 2015.

Hijmans, R. J. and van Etten, J.: raster: Geographic analysis and modeling with raster data. R package version 2.0-12., 2012.

Hooghiemstra, H., Stalling, H., Agwu, C. O. C., and Dupont, L. M.: Vegetational and climatic changes at the northern fringe of the sahara 250,000–5000 years BP: evidence from 4 marine pollen records located between Portugal and the Canary Islands, Rev. Palaeobot. Palynol., 74, 1–53, https://doi.org/10.1016/0034-6667(92)90137-6, 1992.

Hovenden, M. J., Vander Schoor, J. K., and Osanai, Y.: Relative humidity has dramatic impacts on leaf morphology but little effect on stomatal index or density in Nothofagus cunninghamii (Nothofagaceae), Aust. J. Bot., 60, 700, https://doi.org/10.1071/BT12110, 2012.

Jacobs, Z. and Roberts, R. G.: Chapitre III. Datations par OSL avec la technique du grain unique., in: Préhistoire de la région de Rabat-Témara., vol. 3, Rabat, 52–54, 2012.

Jacobs, Z., Roberts, R. G., Nespoulet, R., El Hajraoui, M. A., and Debénath, A.: Single-grain OSL chronologies for Middle Palaeolithic deposits at El Mnasra and El Harhoura 2, Morocco: Implications for Late Pleistocene human–environment interactions along the Atlantic coast of northwest Africa, J. Hum. Evol., 62, 377–394, https://doi.org/10.1016/j.jhevol.2011.12.001, 2012.

Janati-Idrissi, N., Falgueres, C., Nespoulet, R., El Hajraoui, M. A., Debénath, A., Bejjit, L., Bahain, J.-J., Michel, P., Garcia, T., Boudad, L., El Hammouti, K., and Oujaa, A.: Datation

https://doi.org/10.5194/cp-2021-185
Preprint. Discussion started: 5 January 2022

par ESR-U/th combinées de dents fossiles des grottes d'El Mnasra et d'El Harhoura 2, région de Rabat-Temara. Implications chronologiques sur le peuplement du Maroc atlantique au Pléistocène supérieur et son, Quaternaire, 23, 25–35, https://doi.org/10.4000/quaternaire.6127, 2012.

Jeffrey, A.: Exploring palaeoaridity using stable oxygen and carbon isotopes in small mammal teeth: a case study from two Late Pleistocene archaeological cave sites in Morocco, North Africa, 2016.

Jolliffe, I. T. and Cadima, J.: Principal component analysis: a review and recent developments, Philos. Trans. R. Soc. Math. Phys. Eng. Sci., 374, 20150202, https://doi.org/10.1098/rsta.2015.0202, 2016.

Kageyama, M., Braconnot, P., Bopp, L., Caubel, A., Foujols, M.-A., Guilyardi, E., Khodri, M., Lloyd, J., Lombard, F., Mariotti, V., Marti, O., Roy, T., and Woillez, M.-N.: Mid-Holocene and Last Glacial Maximum climate simulations with the IPSL model—part I: comparing IPSL_CM5A to IPSL_CM4, Clim. Dyn., 40, 2447–2468, https://doi.org/10.1007/s00382-012-1488-8, 2013.

Kageyama, M., Albani, S., Braconnot, P., Harrison, S. P., Hopcroft, P. O., Ivanovic, R. F., Lambert, F., Marti, O., Peltier, W. R., Peterschmitt, J.-Y., Roche, D. M., Tarasov, L., Zhang, X., Brady, E. C., Haywood, A. M., LeGrande, A. N., Lunt, D. J., Mahowald, N. M., Mikolajewicz, U., Nisancioglu, K. H., Otto-Bliesner, B. L., Renssen, H., Tomas, R. A., Zhang, Q., Abe-Ouchi, A., Bartlein, P. J., Cao, J., Li, Q., Lohmann, G., Ohgaito, R., Shi, X., Volodin, E., Yoshida, K., Zhang, X., and Zheng, W.: The PMIP4 contribution to CMIP6 – Part 4: Scientific objectives and experimental design of the PMIP4-CMIP6 Last Glacial Maximum experiments and PMIP4 sensitivity experiments, 23, 2017.

Kutzbach, J. E. and Otto-Bliesner, B. L.: The Sensitivity of the African-Asian Monsoonal Climate to Orbital Parameter Changes for 9000 Years B.P. in a Low-Resolution General Circulation Model, J. Atmospheric Sci., 39, 1982.

Le Houérou, H. N.: Climate, flora and fauna changes in the Sahara over the past 500 million years, J. Arid Environ., 37, 619–647, https://doi.org/10.1006/jare.1997.0315, 1997.

Le Mézo, P., Beaufort, L., Bopp, L., Braconnot, P., and Kageyama, M.: From monsoon to marine productivity in the Arabian Sea: insights from glacial and interglacial climates, Clim. Past, 13, 759–778, https://doi.org/10.5194/cp-13-759-2017, 2017.

Lê, S., Josse, J., and Husson, F.: FactoMineR: an R Package for multivariate analysis, J. Stat. Softw., 25, https://doi.org/10.18637/jss.v025.i01, 2008.

Levin, N. E., Cerling, T. E., Passey, B. H., Harris, J. M., and Ehleringer, J. R.: A stable isotope aridity index for terrestrial environments, Proc. Natl. Acad. Sci., 103, 11201–11205, https://doi.org/10.1073/pnas.0604719103, 2006.

Lin, G.: Chapter 4: Research on stable isotope and carbon cycle (1st ed.), in: Stable Isotope Ecology, Beijing, 89–123, 2013.

Lionello, P., Malanotte, P., and Boscolo, R. (Eds.): Mediterranean Climate Variability, Elsevier., Elsevier, Amsterdam, 2006.

Longinelli, A. and Selmo, E.: Isotopic composition of precipitation in Italy: a first overall map, J. Hydrol., 270, 75–88, https://doi.org/10.1016/S0022-1694(02)00281-0, 2003.

Marquer, L., Otto, T., Ben Arous, E., Stoetzel, E., Campmas, E., Zazzo, A., Tombret, O., Falgueres, C., El Hajraoui, M. A., and Nespoulet, R.: Early human use of wild olive during the Aterian Middle Stone Age in North Africa, *in press*.

Marti, O., Braconnot, P., Dufresne, J.-L., Bellier, J., Benshila, R., Bony, S., Brockmann, P., Cadule, P., Caubel, A., Codron, F., de Noblet, N., Denvil, S., Fairhead, L., Fichefet, T., Foujols, M.-A., Friedlingstein, P., Goosse, H., Grandpeix, J.-Y., Guilyardi, E., Hourdin, F., Idelkadi, A., Kageyama, M., Krinner, G., Lévy, C., Madec, G., Mignot, J., Musat, I., Swingedouw, D., and Talandier, C.: Key features of the IPSL ocean atmosphere model and its

https://doi.org/10.5194/cp-2021-185
Preprint. Discussion started: 5 January 2022

sensitivity to atmospheric resolution, Clim. Dyn., 34, 1–26, https://doi.org/10.1007/s00382-009-0640-6, 2010.

Martínez-Blancas, A. and Martorell, C.: Changes in niche differentiation and environmental filtering over a hydric stress gradient, J. Plant Ecol., 13, 185–194, https://doi.org/10.1093/jpe/rtz061, 2020.

Matthews, T.: Predators, prey and the palaeoenvironment., South Afr. J. Sci., 95, 22–24, 2000.

McNeil, J. N.: Behavioral Ecology of Pheromone-Mediated Communication in Moths and Its Importance in the Use of Pheromone Traps, Annu. Rev. Enthomology, 36, 407–30, 1991.

Michel, P., Campmas, É., Stoetzel, E., Nespoulet, R., Abdeljalil El Hajraoui, M., and Amani, F.: La macrofaune du Pléistocène supérieur d'El Harhoura 2 (Témara, Maroc) : données préliminaires, L'Anthropologie, 113, 283–312, https://doi.org/10.1016/j.anthro.2009.04.003, 2009.

Monteith, J. L.: Solar Radiation and Productivity in Tropical Ecosystems, J. Appl. Ecol., 9, 747, https://doi.org/10.2307/2401901, 1972.

Navarro, N., Lécuyer, C., Montuire, S., Langlois, C., and Martineau, F.: Oxygen isotope compositions of phosphate from arvicoline teeth and Quaternary climatic changes, Gigny, French Jura, Quat. Res., 62, 172–182, https://doi.org/10.1016/j.yqres.2004.06.001, 2004.

Nespoulet, R. and El Hajraoui, M. A.: Excavation report, 2012.

O'Leary, M. H.: Carbon Isotopes in Photosynthesis, BioScience, 38, 328–336, https://doi.org/10.2307/1310735, 1988.

Paz, H., Pineda-García, F., and Pinzón-Pérez, L. F.: Root depth and morphology in response to soil drought: comparing ecological groups along the secondary succession in a tropical dry forest, Oecologia, 179, 551–561, https://doi.org/10.1007/s00442-015-3359-6, 2015.

Pellegrino, A. C., Peñaflor, M. F. G. V., Nardi, C., Bezner-Kerr, W., Guglielmo, C. G., Bento, J. M. S., and McNeil, J. N.: Weather Forecasting by Insects: Modified Sexual Behaviour in Response to Atmospheric Pressure Changes, PLoS ONE, 8, e75004, https://doi.org/10.1371/journal.pone.0075004, 2013.

Peters, S. E. and Bork, K. B.: Species-Abundance Models: An Ecological Approach to Inferring Paleoenvironment and Resolving Paleoecological Change in the Waldron Shale (Silurian), PALAIOS, 14, 234, https://doi.org/10.2307/3515436, 1999.

R Development Core Team: R: A language and environment for statistical computing. R Foundation for Statistical Computing, Vienna, Austria. ISBN 3-900051-07-0, URL: http://www.R-project.org., 2018.

Royer, A., Lécuyer, C., Montuire, S., Amiot, R., Legendre, S., Cuenca-Bescós, G., Jeannet, M., and Martineau, F.: What does the oxygen isotope composition of rodent teeth record?, Earth Planet. Sci. Lett., 361, 258–271, https://doi.org/10.1016/j.epsl.2012.09.058, 2013.

Sampson, P. D., Streissguth, A. P., and Bookstein, F. L.: Neurobehavioral Effects of Prenatal Alcohol: Part II. Partial Least Squares Analysis I, Neurotoxicol. Teratol., 11, 477–491, 1989.

Schmidt, G. A., Annan, J. D., Bartlein, P. J., Cook, B. I., Guilyardi, E., Hargreaves, J. C., Harrison, S. P., Kageyama, M., LeGrande, A. N., Konecky, B., Lovejoy, S., Mann, M. E., Masson-Delmotte, V., Risi, C., Thompson, D., Timmermann, A., Tremblay, L.-B., and Yiou, P.: Using palaeo-climate comparisons to constrain future projections in CMIP5, Clim. Past, 10, 221–250, https://doi.org/10.5194/cp-10-221-2014, 2014.

Schulzweida, U.: CDO User Guide (Version 1.9.8), 2019.

Sepulchre, P., Caubel, A., Ladant, J.-B., Bopp, L., Boucher, O., Braconnot, P., Brockmann, P., Cozic, A., Donnadieu, Y., Dufresne, J.-L., Estella-Perez, V., Ethé, C., Fluteau, F., Foujols, M.-A., Gastineau, G., Ghattas, J., Hauglustaine, D., Hourdin, F., Kageyama, M., Khodri, M., Marti, O., Meurdesoif, Y., Mignot, J., Sarr, A.-C., Servonnat, J., Swingedouw, D., Szopa, S., and Tardif, D.: IPSL-CM5A2 – an Earth system model designed for multi-millennial climate

https://doi.org/10.5194/cp-2021-185
Preprint. Discussion started: 5 January 2022

simulations, Geosci Model Dev, 43, 2020.
Smiley, T. M., Cotton, J. M., Badgley, C., and Cerling, T. E.: Small-mammal isotope ecology tracks climate and vegetation gradients across western North America, Oikos, 125, 1100–1109, https://doi.org/10.1111/oik.02722, 2016.
Sobrino, J. A. and Raissouni, N.: Toward remote sensing methods for land cover dynamic monitoring: Application to Morocco, Int. J. Remote Sens., 21, 353–366, https://doi.org/10.1080/014311600210876, 2000.
Stoetzel, E.: Les microvertébrés du site d'occupation humaine d'El Harhoura 2 (Pleistocene supérieur - Holocène, Maroc) : systématique, évolution, taphonomie et paléoécologie., 437, 2009.
Stoetzel, E., Bailon, S., Nespoulet, R., El Hajraoui, M. A., and Denys, C.: Pleistocene and holocene small vertebrates of El Harhoura 2 cave (Rabat–Témara, Morocco): an annotated preliminary taxonomic list, Hist. Biol., 22, 303–319, https://doi.org/10.1080/08912960903461288, 2010.
Stoetzel, E., Marion, L., Nespoulet, R., El Hajraoui, M. A., and Denys, C.: Taphonomy and palaeoecology of the late Pleistocene to middle Holocene small mammal succession of El Harhoura 2 cave (Rabat-Témara, Morocco), J. Hum. Evol., 60, 1–33, https://doi.org/10.1016/j.jhevol.2010.07.016, 2011.
Stoetzel, E., Bougariane, B., Campmas, E., Ouchaou, B., and Michel, P.: Chapitre V. Faunes et paléoenvironnements., in: Préhistoire de la région de Rabat-Témara., vol. 3, Rabat, 35–51, 2012a.
Stoetzel, E., Denys, C., Bailon, S., El Hajraoui, M. A., and Nespoulet, R.: Taphonomic Analysis of Amphibian and Squamate Remains from El Harhoura 2 (Rabat-Témara, Morocco): Contributions to Palaeoecological and Archaeological Interpretations: Taphonomic Study of Amphibian and Squamate Fossil Remains, Int. J. Osteoarchaeol., 22, 616–635, https://doi.org/10.1002/oa.1275, 2012b.
Stoetzel, E., Denys, C., Michaux, J., and Renaud, S.: *Mus* in Morocco: a Quaternary sequence of intraspecific evolution: Quaternary Evolution of *Mus* in Morocco, Biol. J. Linn. Soc., 109, 599–621, https://doi.org/10.1111/bij.12065, 2013.
Stoetzel, E., Campmas, E., Michel, P., Bougariane, B., Ouchaou, B., Amani, F., El Hajraoui, M. A., and Nespoulet, R.: Context of modern human occupations in North Africa: Contribution of the Témara caves data, Quat. Int., 320, 143–161, https://doi.org/10.1016/j.quaint.2013.05.017, 2014.
Stoetzel, E., Cornette, R., Lalis, A., Nicolas, V., Cucchi, T., and Denys, C.: Systematics and evolution of the Meriones shawii/grandis complex (Rodentia, Gerbillinae) during the Late Quaternary in northwestern Africa: Exploring the role of environmental and anthropogenic changes, Quat. Sci. Rev., 164, 199–216, https://doi.org/10.1016/j.quascirev.2017.04.002, 2017.
Streissguth, A. P., Bookstein, F. L., Sampson, P. D., and Barr, H. M.: The enduring effects of prenatal alcohol exposure on child development: Birth through seven years, a partial least squares solution., The University of Michigan Press., 1993.
Tanner, E. V. J., Kapos, V., and Healey, J. R.: Hurricane Effects on Forest Ecosystems in the Caribbean, Biotropica, 23, 513, https://doi.org/10.2307/2388274, 1991.
Tchernov, E.: The Faunal Sequence of the Southwest Asian Middle Paleolithic in Relation to Hominid Dispersal Events, in: Neandertals and Modern Humans in Western Asia, edited by: Akazawa, T., Aoki, K., and Bar-Yosef, O., Kluwer Academic Publishers, Boston, 77–94, https://doi.org/10.1007/0-306-47153-1_6, 2002.
Terray, L., Stoetzel, E., Herrel, A., and Cornette, R.: The contribution of functional traits to the understanding of palaeoenvironmental changes, Biol. J. Linn. Soc., blab057, https://doi.org/10.1093/biolinnean/blab057, 2021.

https://doi.org/10.5194/cp-2021-185
Preprint. Discussion started: 5 January 2022

Tieszen, L. L.: Natural variations in the carbon isotope values of plants: Implications for archaeology, ecology, and paleoecology, J. Archaeol. Sci., 18, 227–248, https://doi.org/10.1016/0305-4403(91)90063-U, 1991.

775 Trauth, M. H., Larrasoaña, J. C., and Mudelsee, M.: Trends, rhythms and events in Plio-Pleistocene African climate, Quat. Sci. Rev., 28, 399–411, https://doi.org/10.1016/j.quascirev.2008.11.003, 2009.

Wei, T. and Simko, V.: R package "corrplot": Visualization of a Correlation Matrix. (Version 0.90), 2021.

780 Wickham, H.: ggplot2: elegant graphics for data analysis., Springer, 2015.

Yom-Tov, Y. and Geffen, E.: Geographic variation in body size: the effects of ambient temperature and precipitation, Oecologia, 148, 213–218, https://doi.org/10.1007/s00442-006-0364-9, 2006.